Int J Clin Exp Med 2018;11(12):13135-13146
www.ijcem.com /ISSN:1940-5901/IJCEM0077643

Original Article

Relationship between expression of myogenic factors in disused rats and bone mass loss and microstructural degeneration

Yan Zhang[1,3,4], Haoliang Xiao[2], Yinghui Zhou[1,3,4], Shuying Liu[1,3,4], Dandan Xie[5], Sang Fu[6], Shanjiang Fu[7], Zhifeng Sheng[1,3,4], Hui Xie[8]

[1]Department of Metabolism and Endocrinology, The Second Xiangya Hospital, Central South University, Changsha 410011, Hunan, China; [2]Laboratory Animal Center, The Second Xiangya Hospital, Central South University, Changsha 410011, Hunan, China; [3]Institution of Metabolism and Endocrinology of Central South University, Changsha 410011, Hunan, China; [4]National Clinical Research Center for Metabolic Diseases, Changsha 410011, Hunan, China; [5]Department of Clinical Nutrition, The Affiliated Hospital of Hainan Medical College, Haikou 570100, Hainan, China; [6]Health Management Center, Xiangtan Central Hospital, Xiangtan 411100, Hunan, China; [7]Department of Metabolism and Endocrinology, The Third People's Hospital of Hainan Province, Sanya 572000, Hainan, China; [8]Movement System Injury and Repair Research Center, Xiangya Hospital, Central South University, Changsha 410008, Hunan, China

Received April 9, 2018; Accepted September 11, 2018; Epub December 15, 2018; Published December 30, 2018

Abstract: Background: Although it has been widely accepted that disuse osteoporosis will lead to changes in myogenic factors and bone metabolism, it is less clear whether myogenic factors are associated with bone mass loss and microstructural degradation. The purpose of this study was to determine the relationship between expression of myogenic factors in disused rats and bone mass loss and microstructural degradation. Methods: Immobilization was induced by injecting Botox into the right hind limb muscles in a Wistar rat model. Before sacrifice, whole body dual energy X-ray absorptiometry (DXA) measurements were taken. Next, DXA and microCT scanning were performed on the right femora *in vitro*. This facilitated the evaluation of numerous bone parameters, including bone mineral density (BMD). BMDs of seven regions in the femora were determined. Serum expression of numerous muscle-bone biochemical markers was quantified through ELISA. Quadriceps femoris tissue expression of important factors was assessed through immunohistochemistry. Correlation analysis was performed to investigate potential mechanisms of muscular atrophy. Results: BTX rats lost a significant amount of body weight in the first two weeks post injection, before regaining weight in accord with controls. Mean lean mass of the BTX group was significantly lower at both two and four weeks. Specific regions in the femora exhibited significantly less BMD than the control group. Trabecular and cortical bone microstructures were significantly different in BTX and control groups. Biochemical analysis revealed differences in seven markers. Correlation analysis revealed that OPG/RANKL pathways may be integral to muscular atrophy. Conclusion: Expression of myogenic factors may be related to loss of bone mass and degeneration of bone microstructures. OPG/RANKL pathways may play a role in its mechanisms.

Keywords: Botox, disuse, loss of bone mass, bone mineral density, bone microstructure

Introduction

Disuse osteoporosis is defined as localized bone loss caused by a reduction in mechanical stress. Loss of mechanical stress on bone induces acceleration of osteoclast-mediated bone resorption and inhibition of osteoblast-mediated bone formation, resulting in overall bone loss [1]. Therapeutic bed rest [2], localized immobilization due to spinal cord injuries [3], and hemiplegia or hemiparesis due to strokes [4] or fractures [5, 6] can lead to disuse osteoporosis. In contrast with primary osteoporosis, the cause of disuse osteoporosis is a lack of muscle movement contraction on the bone, basically a lack of mechanical stimulation [7].

Many studies have suggested that different bones, even the same bones in different areas, have different reactions to bone loss caused by muscle atrophy. Furthermore, the most sensitive skeleton sites to disuse osteoporosis are

the lower limbs, such as knees and ankles [8]. Indeed, a high-content of trabecular bone is more prone to disuse bone loss [1]. In a 17-week bed rest experiment, Leblanc et al. found that bone loss was located significantly in load-bearing bones, while non-bearing bone (such as the skull) mass increased [9]. Few studies have been conducted examining the effects of muscle atrophy on different bone regions. Most studies have only distinguished between trabecular bone and cortical bone regions. In this study, rat femurs were divided equally into seven regions and the bone mineral density was measured in each region, with an aim of determining bone loss sensitive areas in the femur. Moreover, this study assessed bone mass and microstructures of trabecular and cortical bones.

Bones and muscles are two important components of the musculoskeletal system, closely linked and interrelated [10, 11]. Appropriate exercise plays an important role in increasing and maintaining bone mass and bone strength, through the continual application of mechanical stress [12]. Previous studies have reported that muscle influences bone through its contraction. In recent years, it has been found that muscle can also affect bone structure and function through endocrine factors [13]. Several non-mechanical factors contribute to the muscle-bone relationship [13], such as genetic, hormonal, and nutritional factors, including leptin and adiponectin [14], Wnt, PPARγ, and TGFβ signaling pathways [14-16]. The direct cause of disuse osteoporosis is skeletal muscle disuse. Previous studies have only focused on skeletal parameters, such as bone mass, bone microstructure, and osteogenic related factors. Little research has focused on the correlation between osteoporosis and myogenic factors, such as growth differentiation factor-8 (GDF8), fibroblast growth factor 6 (FGF6), or myogenic differentiation protein (MyoD). GDF8 is a member of the TGF-β superfamily and a negative regulator of skeletal muscle mass [17]. FGF-6 belongs to the FGF superfamily and controls cell proliferation, differentiation, and morphogenetic events [18]. MyoD is a member of the basic-helix-loop-helix family of proteins, playing a vital role in the plasticity of skeletal muscles [19, 20]. In this study, expression of myogenic factors in muscle and serum was detected by immunohistochemistry (IHC) and enzyme-linked immunosorbent assays (ELISA).

To explore the correlation between myogenic factors and bone mass and microstructures in disuse osteoporosis, a rat model of osteoporosis was established by intramuscular injection of Botox (BTX). BMD [47] and body components were measured by DXA and microCT. Concentrations of serum myogenic factors and bone turnover factors [21, 22] were determined by ELISA and expression levels of myogenic factors in quadriceps femoris muscles were detected by IHC. Finally, the correlation between myogenic factors and both bone mass and bone microstructure degeneration were analyzed by partial correlation analysis.

Materials and methods

Animal preparation

Forty-two 6-week old female Wistar rats of average body weights (171 ± 5 g) were obtained from the Shanghai Research Center for Biomodel Organisms. After 2 weeks of acclimatization to local conditions (24°C and a 12 h/12-hour light/dark cycle) in the animal house facility of the Second Xiangya Hospital (Central South University, China), the rats were randomly assigned to seven groups of six rats each. On day 0, rats from the 6 groups were weighed and injected intramuscularly with 2 U of BTX (BTX, Institute of Biology, Lanzhou, China) dissolved in 0.4 mL of physiological saline or just saline in the right muscle quadriceps femoris. Rats were weighed on day 1 of every week and sacrificed at 2 weeks, 4 weeks, and 8 weeks by taking blood from the abdominal aorta, after fasting for 8 hours and after full-body dual-energy X-ray absorptiometry (DXA) measurements. The remaining 6 rats were not injected. They were sacrificed on day 0 as the baseline group. For all rats, serum was harvested and stored at -70°C for biochemical analysis. Femora were used for DXA and micro-CT analyses. Right quadriceps femoris muscles were harvested for immunohistochemical analysis. All animal procedures were approved by the Institutional Animal Care and Use Committee of the People's Republic of China.

Biochemical markers

CTX-I, PINP, OPG, RANKL, GDF8, FGF6, and MyoD were detected by ELISA with commercial kits (Nanjing Jiancheng Bioengineering Institute; inter-assay cv < 12% and intra-assay cv < 10%).

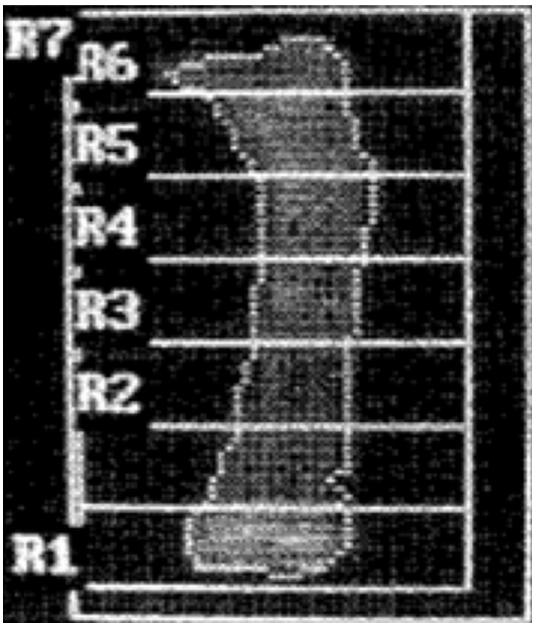

Figure 1. Analysis of isolated tibia in rats by DXA measurements.

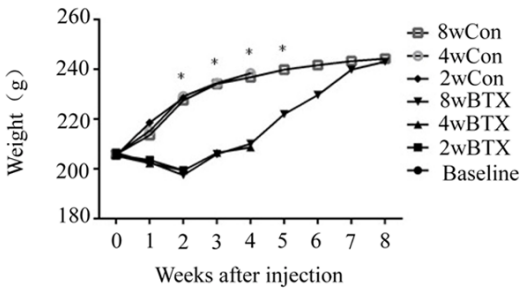

Figure 2. BTX and control group weight variations. BTX-injected rats suffered rapid body weight loss, then slowly regained weight until in accord with controls. *$P < 0.05$ vs. Control group. BTX, BTX group; Con, control group.

Immunohistochemistry (IHC)

The animals were euthanized and right quadriceps femoris muscles were harvested immediately. For IHC analysis, tissue samples were fixed with 10% phosphate-buffered formalin at room temperature for 24 hours. Samples were then dehydrated and embedded in paraffin, while 5-μm-thick cross sections were cut with a microtome and placed on glass slides. Sections were then incubated with primary antibodies for GDF8 (rabbit, 1:200, Santa Cruz Biotechnology, Santa Cruz, CA, USA), FGF6 (rabbit, 1:200, Santa Cruz Biotechnology, Santa Cruz, CA, USA), and MyoD (rabbit, 1:50, Santa Cruz Biotechnology, Santa Cruz, CA, USA) for 2 hours at room temperature. Sections were then rinsed and incubated with polyclonal secondary antibody for 1 hour at room temperature. After extensive rinsing, sections were incubated for 3 minutes with peroxidase streptavidin conjugate and visualized with diaminobenzidine. Negative control slides, with omission of the primary antibodies, were incubated according to immunostaining procedures in each instance.

DXA measurement

Whole bodies and femora of the rats were analyzed using a Hologic QDR-4500A dual-energy X-ray absorptiometry bone densitometer (Hologic; Bedford, MA, USA) under conditions of 41 R and 100 kVP [23]. Scanning widths were 18 cm (for the whole body) and 5 cm (for the femora) and the velocity was 4.8 cm/s. Total body composition was assessed in each of the 42 rats, with rigorous repositioning between scans and without changing calibration for the same rat. Bone mass content (BMC), fat mass (FM), lean mass (LM), and bone mineral density (BMD) were measured. For femora, seven equal lines of the whole length were analyzed, as shown in **Figure 1**. All scans were analyzed with software designed for analysis of small animals. Quality-control scans were performed everyday using the manufacturer-supplied phantom.

MicroCT analysis

MicroCT scanning [24, 25] was performed with a SkyScan scanner and associated software (Skyscan 1176, Bruker micro-CT, Kontich, Belgium). This machine was equipped with an aluminum filter (0.5 mm) to exclude low-energy rays. The scanning protocol was set at X-ray energy settings of 50 kV and 200 μA and each sample was scanned over 1 entire 360° rotation, with an exposure time of 250 ms/frame. An isotopic resolution of 18 μm pixel size that displayed the microstructure of the proximal femur was selected and the angle of increment around the sample was set to 0.4°. X-ray fluoroscopies were performed to correct the placement of each sample within the sample holder and to ensure that the whole sample was included within the scanning field. Histomorphometric analyses were performed using an OsteoMeasure histomorphometry system (OsteoMetrics, Decatur, GA).

Table 1. Measurement of 2D projection DXA

	2 w BTX (n = 6)	2 w Con (n = 6)	4 w BTX (n = 6)	4 w Con (n = 6)	8 w BTX (n = 6)	8 w Con (n = 6)
BMC (g)	6.630 ± 0.6	6.970 ± 0.4	6.687 ± 0.7	7.142 ± 0.2	8.090 ± 0.8	8.297 ± 0.1
BMD (g/cm^2)	0.167 ± 0.0	0.167 ± 0.0	0.174 ± 0.0	0.173 ± 0.0	0.168 ± 0.0	0.174 ± 0.0
FM (g)	36.917 ± 7.6	43.267 ± 7.7	36.533 ± 8.7	44.033 ± 3.1	41.267 ± 4.5	37.217 ± 3.0
LM (g)	135.383 ± 11.7*	157.233 ± 3.6	146.167 ± 10.5*	166.167 ± 4.7	156.850 ± 5.2	163.250 ± 3.5

*$P < 0.05$ vs. Control group. BMC, bone mineral content; BMD, bone mineral density; FM, fat mass; LM, lean mass; w, weeks; BTX, BTX group; Con, control group. Data are shown as mean ± SD.

Table 2. Changes in bone mineral density in different regions of rat femora

Regions	2 w BTX (n = 6)	2 w Con (n = 6)	4 w BTX (n = 6)	4 w Con (n = 6)	8 w BTX (n = 6)	8 w Con (n = 6)
ROI1	0.236 ± 0.0*	0.265 ± 0.0	0.233 ± 0.0*	0.277 ± 0.0	0.248 ± 0.0*	0.272 ± 0.0
ROI2	0.180 ± 0.0*	0.208 ± 0.0	0.180 ± 0.0*	0.204 ± 0.0	0.179 ± 0.0*	0.205 ± 0.0
ROI3	0.148 ± 0.0	0.163 ± 0.0	0.151 ± 0.0	0.171 ± 0.0	0.156 ± 0.0*	0.165 ± 0.0
ROI4	0.148 ± 0.0	0.154 ± 0.0	0.149 ± 0.1	0.171 ± 0.0	0.162 ± 0.0	0.171 ± 0.0
ROI5	0.165 ± 0.0	0.172 ± 0.0	0.180 ± 0.0	0.195 ± 0.0	0.176 ± 0.0*	0.181 ± 0.0
ROI6	0.194 ± 0.0	0.204 ± 0.0	0.196 ± 0.1	0.224 ± 0.0	0.199 ± 0.0*	0.204 ± 0.0
ROI7	0.188 ± 0.0*	0.199 ± 0.0	0.190 ± 0.0*	0.218 ± 0.0	0.196 ± 0.0*	0.202 ± 0.0

*$P < 0.05$ vs. Control group. ROI, region of interest. 2 w, 2 weeks; 4 w, 4 weeks; 8 w, 8 weeks. w, weeks; BTX, BTX group; Con, control group. Data are shown as mean ± SD.

Table 3. Microstructural analysis of femora trabeculae in different groups

	2 w BTX (n = 6)	2 w Con (n = 6)	4 w BTX (n = 6)	4 w Con (n = 6)	8 w BTX (n = 6)	8 w Con (n = 6)
tBMD (mg/mm^3)	221.2 ± 3.4*	245.6 ± 5.6	212.9 ± 9.1*	245.6 ± 4.4	240.8 ± 1.2	257.5 ± 1.5
BV/TV (%)	41.7 ± 4.9	46.8 ± 3.4	27.2 ± 7.0	40.6 ± 2.4	22.7 ± 4.7	41.7 ± 5.6
Tb.Th (mm)	0.131 ± 0.0	0.126 ± 0.0	0.113 ± 0.1*	0.123 ± 0.1	0.111 ± 0.0*	0.128 ± 0.0
Tb.Sp (mm)	0.184 ± 0.0	0.165 ± 0.0	0.246 ± 0.0*	0.190 ± 0.0	0.296 ± 0.1*	0.193 ± 0.0
Tb.N (mm)	3.20 ± 0.3*	3.71 ± 0.1	2.39 ± 0.4*	3.29 ± 0.1	2.03 ± 0.3*	3.25 ± 0.3
SMI	1.19 ± 0.2	1.04 ± 0.2	1.90 ± 0.3*	1.35 ± 0.1	2.11 ± 0.2*	1.28 ± 0.3

*$P < 0.05$ vs. Control group. tBMD, tissue bone mineral density; BV/TV, bone volume fraction. Tb.Th, trabecular thickness; Tb.Sp, trabecular separation; Tb.N, trabecular number; SMI, structure model index. w, weeks; BTX, BTX group; Con, control group. Data are shown as mean ± SD.

Table 4. Microstructural analysis of femoral cortex in different groups

	2 w BTX (n = 6)	2 w Con (n = 6)	4 w BTX (n = 6)	4 w Con (n = 6)	8 w BTX (n = 6)	8 w Con (n = 6)
tBMD (mg/mm^3)	549.2 ± 4.1	543.3 ± 1.7	562.5 ± 2.5	558.3 ± 4.5	584.2 ± 2.9	579.9 ± 1.3
BV/TV (%)	87.1 ± 0.2	87.4 ± 0.3	87.1 ± 0.5*	88.0 ± 0.3	88.2 ± 0.3	88.5 ± 0.4
Ct.Th (mm)	0.481 ± 0.0*	0.507 ± 0.0	0.488 ± 0.0*	0.545 ± 0.1	0.540 ± 0.0*	0.573 ± 0.0
Ct.Po (%)	12.9 ± 0.2	12.6 ± 0.6	12.9 ± 0.5*	12.0 ± 0.3	11.8 ± 0.3	11.5 ± 0.4

*$P < 0.05$ vs. Control group. tBMD, tissue bone mineral density; BV/TV, bone volume fraction. Ct.Th, cortical thickness; Ct.Po, cortical porosity. w, weeks; BTX, BTX group; Con, control group. Data are shown as mean ± SD.

In the case of the femora, trabecular bone analysis was performed in the volume of interest (VOI), commencing about 1.65 mm (92 image slices) from the growth plate level in the direction of the metaphysis and extending from this position for another 2 mm (112 image slices). The cortical region commenced about 10.5 mm (586 image slices) from the growth plate level

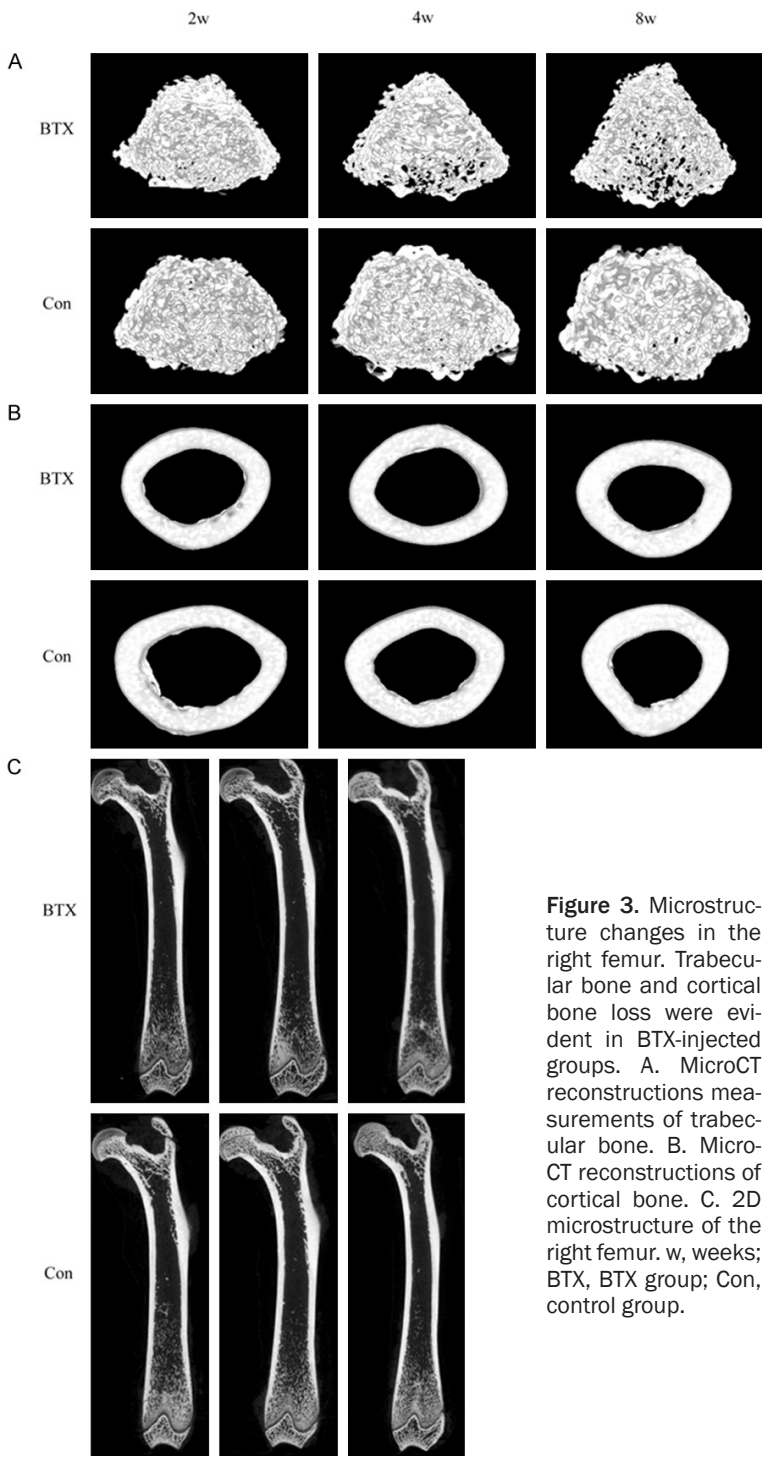

Figure 3. Microstructure changes in the right femur. Trabecular bone and cortical bone loss were evident in BTX-injected groups. A. MicroCT reconstructions measurements of trabecular bone. B. MicroCT reconstructions of cortical bone. C. 2D microstructure of the right femur. w, weeks; BTX, BTX group; Con, control group.

in the direction of the metaphysis and extended from this position for another 0.75 mm (42 image slices).

Several bone parameters were measured: (1) Tissue BMD, representing the BMD at the tissue level and defined as the tissue mineral content divided by the volume of the above-threshold voxels; (2) Bone volume fraction (BV/TV); (3) Trabecular thickness (Tb.Th); (4) Trabecular separation (Tb.Sp); (5) Trabecular number (Tb.N); (6) Structure model index (SMI); (7) Cortical bone thickness (Ct.Th); and (8) Cortical bone porosity (Ct.Po).

Statistics

Statistical analysis was performed using SPSS 13.0 for Windows statistical software (SPSS, Chicago, IL, USA). Analysis of variance (ANOVA) was used to compare mean values from different groups. Correlation between myogenic factors and microstructural parameters was evaluated. Significance is set at $P < 0.05$.

Results

General findings

Twenty-four hours after BTX injections, all rats exhibited lameness and hind limb abduction during tail suspension and toe extension. Signs of lameness reached a maximum 48 hours after injection. **Figure 2** shows that BTX-injected rats suffered rapid body weight loss in the first 2 weeks, before slowly regaining weight in accord with controls. At any time-point, the mean body weight of the BTX group was lower than the control group, significantly between 2 and 4 weeks ($P < 0.05$).

DXA measurements of total body composition

All data are represented as mean plus standard deviation (SD), as shown in **Table 1**. After injections of BTX, only LM was significantly lower, compared to the control group, at weeks 2 (14%) and 4 (12%), then converging to level

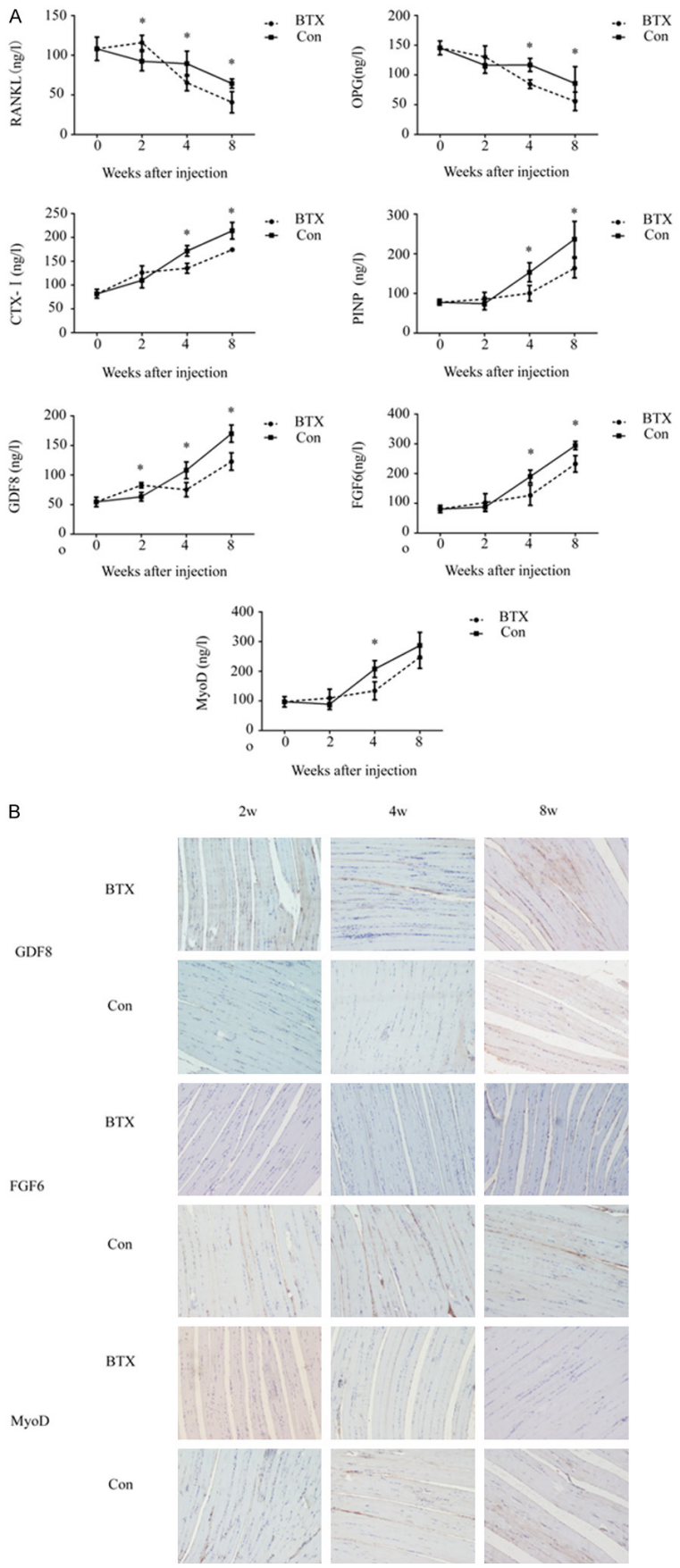

Figure 4. Myogenic factor changes in rats at different time points. GDF8 was increased while FGF6 and MyoD were decreased in BTX-injected groups.*$P < 0.05$ vs. Control group. A. Changes in circular myogenic factors, bone turnover markers and OPG/RANKL in rats at different time points. B. Immunoexpression of GDF8, FGF6, and MyoD in rat right quadriceps tissue (10x). Positive cells are stained brown. CTX-I, collagen type I cross-linked C-telopeptide; PINP, N-terminal propeptide of procollagen type I; RANKL, receptor activator for nuclear factor-κ B ligand; OPG, osteoprotegerin; GDF8, growth differentiation factor-8; MyoD, myogenic differentiation protein; FGF6, fibroblast growth factor-6; w, weeks; BTX, BTX group; Con, control group.

with the control group by week 8.

DXA measurements of femora

As shown in **Table 2**, at weeks 2 and 4, the right femoral BMDs of ROI 1, 2, and 7 in the BTX group were significantly lower than the control group. By week 8, the right femoral BMDs of ROI 1, 2, 3, 5, 6, and 7 in the BTX group were significantly lower than the control group.

MicroCT analysis

Tissue BMD and microstructural parameters of trabecular bone and cortical bone in the femur metaphysis at weeks 2, 4, and 8 are summarized in **Tables 3** and **4**, respectively. Trabecular bone loss is also evident in **Figure 3**. At the proximal femora metaphysis, trabecular bone and cortical bone microstructure were affected by BTX. Regarding the trabecular bone in the BTX group, tBMD and Tb.N were significantly diminished, compared to control rats, at week

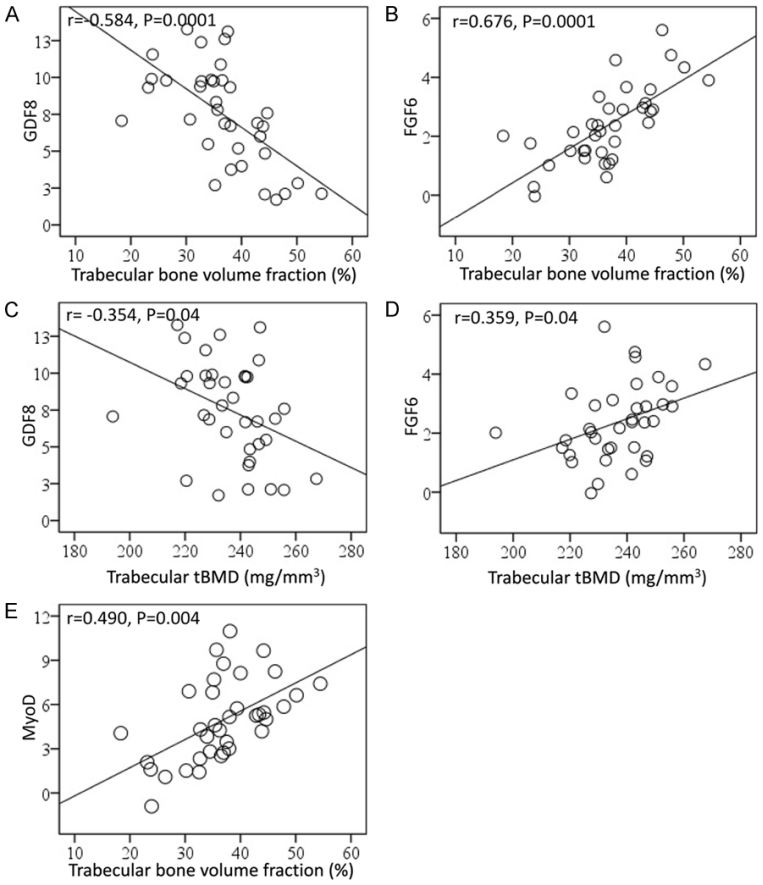

Figure 5. Partial correlation analysis between myogenic factors and bone mass (adjusted for lean mass, fat mass, and age). GDF8 was negatively correlated while FGF6 and MyoD were positively correlated with trabecular bone mass and bone microstructure. GDF8, growth differentiation factor-8; MyoD, myogenic differentiation protein; FGF6, fibroblast growth factor-6. tBMD, tissue bone mineral density; BV/TV, bone volume fraction. A. y = 17.09 - 0.26x, r = -0.584 ($P < 0.01$); B. y = -1.91 + 0.12x, r = 0.676 ($P < 0.01$); C. y = 28.59 - 0.09x, r = -0.354 ($P < 0.05$); D. y = -5.88 + 0.03x, r = 0.359 ($P < 0.05$); E. y = -2.11 + 0.19x, r = 0.490 ($P < 0.01$); BTX, BTX group; Con, control group.

2 (-9.8%, -13.5%). Four weeks after BTX injections, tissue BMD (13.4%), BV/TV (33.0%), Tb.Th (8.1%), and Tb.N (27.4%) had all decreased significantly ($P < 0.05$), while Tb.Sp and SMI increased by 29.5% and 40.7%, compared to the control group ($P < 0.05$). After 8 weeks, changes were in accord with those found at week 4, except for tissue BMD which was similar for both BTX injected and control rats.

For cortical bone, Ct.Th was significantly lower for BTX injected limbs during the experiment, reaching -5.1% by week 2, -10.5% by week 4, and -5.8% by week 8, compared to the control group. Equally, Ct.Po was significantly increased (8.3%) by week 4.

Biochemical analysis

Biochemical analysis revealed differences in seven markers. Results are summarized in **Figure 4A**. Serum RANKL and GDF8 increased in BTX-injected rats from baseline to levels that were significantly higher than those observed for the control group at week 2. These then quickly decreased to levels below the control group. Levels of serum P1NP, CTX-I, OPG, FGF6, and MyoD in BTX-injected rats were higher after 2 weeks than in the control group, but not significantly so. These levels decreased as time progressed to become lower than the controls.

Immunohistochemistry

Expression levels of GDF8, FGF6, and MyoD were detected in the nuclei of cells (**Figure 4B**). In the BTX group, GDF8 increased while FGF6 and MyoD decreased, compared to the control group. There were no significant differences within the BTX group over time.

Partial correlation analysis

Correlation between myogenic factors and microstructural parameters of the right femora is depicted and detailed in **Figure 5** and **Table 5**. After adjustment for lean mass, fat mass, and age, GDF8 was positively correlated with Tb.Sp (r = 0.491, $P < 0.01$) and SMI (r = 0.568, $P < 0.01$), while it was negatively correlated with trabecular tissue BMD (r = -0.354, $P = 0.001$) and BV/TV (r = -0.584, $P = 0.04$), as well as Tb.Th, Tb.N, and Ct.Th (r = -0.516, r = -0.560, and r = -0.553, all $P < 0.01$). Conversely, FGF6 was negatively correlated with Tb.Sp (r = -0.635, $P < 0.01$) and SMI (r = -0.661, $P < 0.01$), while it was positively correlated with trabecular tissue BMD (r = 0.395, $P = 0.001$) and BV/TV (r = 0.676, $P = 0.04$), as well as Tb.Th, Tb.N,

Table 5. Partial correlation analysis between myogenic factors and bone microstructural parameters (adjusted for lean mass, fat mass, and age)

	GDF8	FGF6	MyoD
Tb.Th	-.516**	.592**	.475**
Tb.Sp	.491**	-.635**	-.467**
Tb.N	-.560**	.671**	.477**
SMI	.568**	-.661**	-.443*
Ct.Th	-.553**	.569**	.463**
Ct.Po	.248	-.293	-.181

*$P < 0.05$, **$P < 0.01$. GDF8, Growth differentiation factor-8; MyoD, myogenic differentiation protein; FGF6, fibroblast growth factor-6. Tb.Th, trabecular thickness; Tb.Sp, trabecular separation; Tb.N, trabecular number; SMI, structure model index. Ct.Th, cortical thickness; Ct.Po, cortical porosity.

Table 6. Partial correlation analysis between myogenic factors and bone microstructural parameters (adjusted for lean mass, fat mass, age, and OPG/RANKL)

	GDF8	FGF6	MyoD
Tb.Th	-.250	.390*	.230
Tb.Sp	.268	-.483**	-.256
Tb.N	-.340	.522**	.255
SMI	.369*	-.509**	-.206
Ct.Th	-.340	.421**	.286
Ct.Po	-.037	-.069	.066

*$P < 0.05$, **$P < 0.01$. GDF8, Growth differentiation factor-8; MyoD, myogenic differentiation protein; FGF6, fibroblast growth factor-6. Tb.Th, trabecular thickness; Tb.Sp, trabecular separation; Tb.N, trabecular number; SMI, structure model index. Ct.Th, cortical thickness; Ct.Po, cortical porosity.

Table 7. Partial correlation analysis between myogenic factors and bone turnover markers (adjusted for lean mass, fat mass, and age)

	GDF8	FGF6	MyoD
CTX-I	-.574**	.531**	.609**
PINP	-.618**	.516**	.534**

**$P < 0.01$. GDF8, Growth differentiation factor-8; MyoD, myogenic differentiation protein; FGF6, fibroblast growth factor-6. CTX-I, collagen type I cross-linked C-telopeptide; PINP, N-terminal propeptide of procollagen type I.

and Ct.Th (r = 0.592, r = 0.671, and r = 0.569, all $P < 0.01$). For MyoD, changes were like those found for FGF6, except no correlation was found between trabecular tissue BMD and MyoD.

After adjustment for lean mass, fat mass, age, and serum OPG and RANKL (**Table 6**), partial correlation analyses had changed, except for FGF6. Specifically, GDF8 was only positively correlated with SMI (r = 0.369, $P < 0.01$) and no correlation was found with MyoD and any microstructural parameters.

It was also found that GDF8 negatively correlated with CTX-I (r = -0.574, $P < 0.01$) and PINP (r = -0.618, $P < 0.01$), while FGF6 and MyoD positively correlated with CTX-I (r = 0.531, r = 0.516, both P < 0.01) and PINP (r = 0.609, r = 0.534, both P < 0.01), after adjustment for lean mass, fat mass, and age (**Table 7**).

Discussion

The present study showed that intramuscular injections of BTX, with a dose of 2 U, were enough to induce localized paralysis in Wistar rats, consistent with previous studies. Weights of BTX injected Wistar rats decreased rapidly for the first 2 weeks, until a minimum was reached. Afterward, the rats slowly regained weight and partial function of the injected limb. This was also consistent with previous studies [26, 27]. No significant differences were found in total body composition BMC, BMD, or fat mass, at any time-point. This suggests that the decrease in body weight was mainly caused by lean mass loss.

To determine bone loss prone areas of the femur, seven regions of the femur were scanned by DXA. It was found that ROI1, ROI2, and ROI7 were the most sensitive regions to muscle atrophy, evidenced by significantly decreased BMD. No significant differences in BMD were found at ROI4 between the BTX group and the control group. ROI1, ROI2, and ROI7 of the femur were mainly trabecular bone (the closer the location to the middle part of the bone, the higher proportion of cortical bone). This suggests that the response of trabecular bone to muscle atrophy is more sensitive than cortical bone. Warner et al. developed a mouse model of unilateral transient hind limb muscle paralysis and found that BV/TV was reduced within the distal femoral epiphysis and proximal tibial metaphysis of BTX injected limbs (-43.2% and -54.3% respectively). Furthermore, they found that BTX treatment significantly diminished Tb.Th (24.8%) and Ct.Th (16.2%) [28]. A study by Poliachik et al., concerning a single injection of BTX into the right calf muscle of a mouse model, showed that tra-

becular degradation within the proximal tibia metaphysis occurred more rapidly than in cortical bone. Maximal bone loss was reached by day 12 with only limited recovery by day 84, while cortical bone volume degradation was maximal on day 28 but had completely recovered by day 84 [29]. These studies are consistent with present findings, in that trabecular bone and cortical bone were affected differently by muscle atrophy. In the present study, trabecular bone degeneration was first identified at week 2 and aggravated by week 4. Even though rat activity was totally recovered by week 8, trabecular bone mass and microstructural parameters were intensely degenerated. Cortical bone degeneration was maximal at week 4 and greatly recovered by week 8. Clearly, trabecular bone and cortical bone have different sensitivities to muscle atrophy. Specifically, trabecular degeneration will occur more rapidly, to a more serious degree, while degeneration lasts longer and recovery is slower.

Previous studies have shown that disuse osteoporosis not only causes bone mass loss and microstructural degeneration [26], but also induces changes in bone turnover markers and myogenic factors [30, 31]. It has been established that CTX-I and PINP are markers of bone resorption and formation, respectively [32-34]. Present results showed that serum CTX-I and PINP in the BTX group were significantly lower at weeks 4 and 8, compared to the control group, suggesting that bone formation and resorption were reduced in this model. In a disuse osteoporosis model made by sciatic neurectomy in the tibia, serum CTX-I levels were dramatically elevated by disuse after 2 weeks and had recovered to normal levels by week 8 [35]. One possible explanation for such variability is that different osteoporosis models have different impacts on serum CTX-I. RANKL is a cytokine that belongs to the TNF family. OPG is also a TNF family member that binds to RANKL and then inhibits the binding of RANKL to RANK [36]. The activity of osteoclasts is highly dependent on the balance between RANKL and OPG. Present results showed that expression of OPG decreased in BTX rats after muscle atrophy, while expression of RANKL increased by week 2 and then decreased quickly by weeks 4 and 8. While no previous studies have reported on changes in serum OPG and RANKL in a BTX-induced osteoporosis model, there are similar tissue related reports. A recent study reported that RANKL levels significantly increased in the proximal tibia 7 days after BTX injections, while OPG levels did not [37]. Lunam et al. demonstrated that, 7 to 14 days after BTX injection into the right quadriceps, gene expression of RANKL was upregulated in the femoral bone marrow [31]. Present results are in accord with these related studies, though further research is warranted to elaborate the mechanisms of RANKL/OPG changes in a disuse osteoporosis model.

Satellite cells are the only source of regenerative repair after muscle injuries. The regeneration process can be divided into migration, proliferation, differentiation, and maturation steps [38]. GDF8 is a TGFβ family-specific growth factor specifically expressed in the skeletal muscle of vertebrates. It inhibits the proliferation and differentiation of muscle cells and inhibits muscle formation [39]. It can also downregulate MyoD expression through the smad3 pathway [40, 41]. In addition to negative regulatory muscle formation, GDF8 can also affect bone structure and bone formation after fractures [42, 43]. MyoD can stimulate the differentiation of multiple types of cells into myoblasts and promote myoblast fusion into myotubes [19, 20]. FGF6 belongs to the FGF family, which can promote the proliferation and differentiation of muscle satellite cells to promote normal skeletal muscle regeneration [18]. Although it has been reported that no significant effects were found on muscle and bone through lack of FGF6 in FGF6 knockout mice, the capacity of muscle regeneration after injury was weakened [44]. GDF8, FGF6, and MyoD mainly act on muscle tissue, although no reports were found concerning the three factors in relation to disuse osteoporosis and circulating serum. In this study, GDF8 serum concentrations were significantly higher in the BTX group than in the control group, at 2 weeks post-injection. However, by 4 and 8 weeks, levels were significantly lower than the control group. FGF6 and MyoD levels in the BTX group were significantly lower after 4 and 8 weeks than the control group. Kunihiro Sakuma et al. reported that, after nerve denervation in Wistar rats, GDF8 expression in fast muscle increased and FGF6 expression decreased [39]. Furthermore, expression of MyoD was reportedly reduced in the gastroc-

nemius of Wistar rats after nerve denervation [45]. These results are consistent with present results. Immunohistochemistry staining showed that, in quadriceps femoris muscles, expression of GDF8 increased while MyoD and FGF6 decreased after BTX injections. Possible causes of the above results were: 1) Rats used in this experiment were in the growth period, thus the muscle tissue growth and corresponding myogenic factor secretions were active; 2) Injection of BTX to the rats was applied on one side of the hind limbs, other parts of the body may have responded in a compensatory manner; and 3) Regeneration after muscle injuries involves multiple processes, not a single one.

To further elaborate the mechanisms underpinning disuse osteoporosis, correlation between myogenic factors and bone mass and microstructure was analyzed by partial correlation analysis. Previous studies have shown that BMD is positively correlated with body weight and negatively correlated with age [42, 46]. Weight mainly includes bone mass, lean mass, and fat mass, with the latter two taking up about 95% of the whole weight [11]. To eliminate the effects of age and weight, analysis was adjusted to account for the lean mass, fat mass, and age of rats. After adjusting, GDF8 was positively correlated with Tb.Sp and SMI, but negatively correlated with trabecular bone tBMD, BV/TV, Tb.Th, Tb.N, and Ct.Th. FGF6 and MyoD were positively correlated with BV/TV, Tb.Th, Tb.N, and Ct.Th, but negatively correlated with Tb.Sp and SMI. No correlation was found between myogenic factors and cortical bone microstructure parameters. Results suggest that expression of GDF8 in tissue was negatively correlated and FGF6 and MyoD expression was positively correlated with trabecular bone mass.

This study further analyzed the correlation between tissue myogenic factors (GDF8, FGF6, and MyoD) and serum bone turnover markers (CTX-I and PINP). After adjustment for lean mass, fat mass, and age, GDF8 was negatively correlated with CTX-I and PINP, while FGF6 and MyoD were positively correlated with CTX-I and PINP. Results suggest that GDF8 was negatively correlated and FGF6 and MyoD were positively correlated with bone formation and resorption.

To further investigate if bone degeneration caused by muscular atrophy is regulated by OPG/RANKL pathways in disuse osteoporosis, partial correlation analysis was additionally adjusted by serum OPG and RANKL. Expectedly, correlation between myogenic factors and trabecular bone and cortical bone considerably changed. Correlation with trabecular bone was weakened and almost no correlation was found with cortical bone, suggesting that OPG/RANKL pathways may be involved in the regulation of bone mass and bone microstructural degeneration caused by muscle atrophy.

In summary, trabecular bone and cortical bone have different sensitivities to muscle atrophy. Specifically, trabecular degeneration occurs more rapidly and seriously, while degeneration lasts longer and the recovery is slower. Quadriceps GDF8 was negatively correlated and FGF6 and MyoD were positively correlated with trabecular bone mass and bone microstructure. OPG/RANKL pathways may be a potential way to regulate bone mass and bone microstructural degeneration caused by muscle atrophy.

Acknowledgements

This work was supported by grants from the National Nature Science Foundation of China [grant number 81471091 and 81870622] and the Hunan Nature Science Foundation [grant number 2018JJ2574].

Disclosure of conflict of interest

None.

Address correspondence to: Zhifeng Sheng, Department of Metabolism and Endocrinology, The Second Xiangya Hospital, Central South University, Renmin Road 139#, Changsha 410011, Hunan, China. Tel: +86-0731-85292152; Fax: +86-13574806523; E-mail: shengzhifeng@csu.edu.cn; Hui Xie, Movement System Injury and Repair Research Center, Xiangya Hospital, Central South University, Xiangya Road 88#, Changsha 410008, Hunan, China. Tel: +86-0731-84327068; E-mail: huixie@csu.edu.cn

References

[1] Takata S and Yasui N. Disuse osteoporosis. J Med Invest 2001; 48: 147-156.

[2] Arnaud SB, Sherrard DJ, Maloney N, Whalen RT and Fung P. Effects of 1-week head-down tilt bed rest on bone formation and the calcium

endocrine system. Aviat Space Environ Med 1992; 63: 14-20.
[3] Leslie WD and Nance PW. Dissociated hip and spine demineralization: a specific finding in spinal cord injury. Arch Phys Med Rehabil 1993; 74: 960-964.
[4] Iversen E, Hassager C and Christiansen C. The effect of hemiplegia on bone mass and soft tissue body composition. Acta Neurol Scand 1989; 79: 155-159.
[5] Kannus P, Jarvinen M, Sievanen H, Oja P and Vuori I. Osteoporosis in men with a history of tibial fracture. J Bone Miner Res 1994; 9: 423-429.
[6] Ceroni D, Martin XE, Delhumeau C, Farpour-Lambert NJ, De Coulon G, Dubois-Ferrière V, Rizzoli R. Recovery of decreased bone mineral mass after lower-limb fractures in adolescents. J Bone Joint Surg Am 2013; 95: 1037-1043.
[7] Iwamoto J. [A role of exercise and sports in the prevention of osteoporosis.] Clin Calcium 2017; 27: 17-23.
[8] Giannotti S, Bottai V, Dell'osso G, De Paola G, Bugelli G, Pini E and Guido G. Disuse osteoporosis of the upper limb: assessment of thirty patients. Clin Cases Miner Bone Metab 2013; 10: 129-132.
[9] Leblanc AD, Schneider VS, Evans HJ, Engelbretson DA and Krebs JM. Bone mineral loss and recovery after 17 weeks of bed rest. J Bone Miner Res 1990; 5: 843-850.
[10] Deng FY, Xiao P, Lei SF, Zhang L, Yang F, Tang ZH, Liu PY, Liu YJ, Recker RR and Deng HW. Bivariate whole genome linkage analysis for femoral neck geometric parameters and total body lean mass. J Bone Miner Res 2007; 22: 808-816.
[11] Wu S, Lei SF, Chen XD, Tan LJ, Jian WX, Deng FY, Sun X, Xiao SM, Jiang C, Guo YF, Zhu XZ and Deng HW. The contributions of lean tissue mass and fat mass to bone geometric adaptation at the femoral neck in Chinese overweight adults. Ann Hum Biol 2007; 34: 344-353.
[12] Handoll HH, Gillespie WJ, Gillespie LD and Madhok R. Moving towards evidence-based healthcare for musculoskeletal injuries: featuring the work of the cochrane bone, joint and muscle trauma group. J R Soc Promot Health 2007; 127: 168-173.
[13] Zhang ZL, He JW, Qin YJ, Hu YQ, Li M, Liu YJ, Zhang H and Hu WW. Association between SNP and haplotypes in PPARGC1 and adiponectin genes and bone mineral density in Chinese nuclear families. Acta Pharmacol Sin 2007; 28: 287-295.
[14] Zhou S, Eid K and Glowacki J. Cooperation between TGF-beta and Wnt pathways during chondrocyte and adipocyte differentiation of human marrow stromal cells. J Bone Miner Res 2004; 19: 463-470.
[15] Karasik D and Kiel DP. Evidence for pleiotropic factors in genetics of the musculoskeletal system. Bone 2010; 46: 1226-1237.
[16] Reid IR. Relationships between fat and bone. Osteoporos Int 2008; 19: 595-606.
[17] Latres E and Mastaitis J. Activin a more prominently regulates muscle mass in primates than does GDF8. Nat Commun 2017; 8: 15153.
[18] Floss T, Arnold HH and Braun T. A role for FGF-6 in skeletal muscle regeneration. Genes Dev 1997; 11: 2040-2051.
[19] Ishido M, Kami K and Masuhara M. In vivo expression patterns of MyoD, p21, and Rb proteins in myonuclei and satellite cells of denervated rat skeletal muscle. Am J Physiol Cell Physiol 2004; 287: C484-493.
[20] Edmondson DG and Olson EN. Helix-loop-helix proteins as regulators of muscle-specific transcription. J Biol Chem 1993; 268: 755-758.
[21] Wu XY, Zhang H, Xie H, Luo XH, Peng YQ, Yuan LQ, Dai RC, Sheng ZF, Wu XP and Liao EY. Reference intervals of bone turnover markers determined by using their curve-fitting valley for adult females in China. Osteoporos Int 2014; 25: 943-952.
[22] Wu XY, Wu XP, Xie H, Zhang H, Peng YQ, Yuan LQ, Su X, Luo XH and Liao EY. Age-related changes in biochemical markers of bone turnover and gonadotropin levels and their relationship among Chinese adult women. Osteoporos Int 2010; 21: 275-285.
[23] Sheng Z, Tong D, Ou Y, Zhang H, Zhang Z, Li S, Zhou J, Zhang J and Liao E. Serum sclerostin levels were positively correlated with fat mass and bone mineral density in central south Chinese postmenopausal women. Clin Endocrinol (Oxf) 2012; 76: 797-801.
[24] Sheng ZF, Ye W, Wang J, Li CH, Liu JH, Liang QC, Li S, Xu K and Liao EY. OPG knockout mouse teeth display reduced alveolar bone mass and hypermineralization in enamel and dentin. Arch Oral Biol 2010; 55: 288-293.
[25] Liu SP, Liao EY, Chen J, Yang SM, Li JW, Sheng ZF, Mo H, Wu XP, Yao L and Dai RC. Effects of methylprednisolone on bone mineral density and microarchitecture of trabecular bones in rats with administration time and assessed by micro-computed tomography. Acta Radiol 2009; 50: 93-100.
[26] Chappard D, Chennebault A, Moreau M, Legrand E, Audran M and Basle MF. Texture analysis of X-ray radiographs is a more reliable descriptor of bone loss than mineral content in a rat model of localized disuse induced by the Clostridium botulinum toxin. Bone 2001; 28: 72-79.

[27] Warner SE, Sanford DA, Becker BA, Bain SD, Srinivasan S and Gross TS. Botox induced muscle paralysis rapidly degrades bone. Bone 2006; 38: 257-264.
[28] Morey-Holton ER and Globus RK. Hindlimb unloading of growing rats: a model for predicting skeletal changes during space flight. Bone 1998; 22: 83s-88s.
[29] Poliachik SL, Bain SD, Threet D, Huber P and Gross TS. Transient muscle paralysis disrupts bone homeostasis by rapid degradation of bone morphology. Bone 2010; 46: 18-23.
[30] Sinningen K, Albus E, Thiele S, Grossklaus S, Kurth T, Udey MC, Chavakis T, Hofbauer LC and Rauner M. Loss of milk fat globule-epidermal growth factor 8 (MFG-E8) in mice leads to low bone mass and accelerates ovariectomy-associated bone loss by increasing osteoclastogenesis. Bone 2015; 76: 107-114.
[31] Marchand-Libouban H, Le Drévo MA, Chappard D. Disuse induced by botulinum toxin affects the bone marrow expression profile of bone genes leading to a rapid bone loss. J Musculoskelet Neuronal Interact 2013; 13: 27-36.
[32] Rosen HN, Moses AC, Garber J, Iloputaife ID, Ross DS, Lee SL and Greenspan SL. Serum CTX: a new marker of bone resorption that shows treatment effect more often than other markers because of low coefficient of variability and large changes with bisphosphonate therapy. Calcif Tissue Int 2000; 66: 100-103.
[33] Khosla S, Burr D, Cauley J, Dempster DW, Ebeling PR, Felsenberg D, Gagel RF, Gilsanz V, Guise T, Koka S, McCauley LK, McGowan J, McKee MD, Mohla S, Pendrys DG, Raisz LG, Ruggiero SL, Shafer DM, Shum L, Silverman SL, Van Poznak CH, Watts N, Woo SB and Shane E. Oral bisphosphonate-induced osteonecrosis: risk factors, prediction of risk using serum CTX testing, prevention, and treatment. J Oral Maxillofac Surg 2008; 66: 1320-1321.
[34] Garnero P. The utility of biomarkers in osteoporosis management. Mol Diagn Ther 2017; 21: 401-418.
[35] Sun X, Yang K, Wang C, Cao S, Merritt M, Hu Y and Xu X. Paradoxical response to mechanical unloading in bone loss, microarchitecture, and bone turnover markers. Int J Med Sci 2015; 12: 270-279.
[36] Lau RY and Guo X. A review on current osteoporosis research: with special focus on disuse bone loss. J Osteoporos 2011; 2011: 293808.
[37] Aliprantis AO, Stolina M, Kostenuik PJ, Poliachik SL, Warner SE, Bain SD and Gross TS. Transient muscle paralysis degrades bone via rapid osteoclastogenesis. FASEB J 2012; 26: 1110-1118.
[38] Yusuf F and Brand-Saberi B. Myogenesis and muscle regeneration. Histochem Cell Biol 2012; 138: 187-199.
[39] Sakuma K, Watanabe K, Sano M, Uramoto I and Totsuka T. Differential adaptation of growth and differentiation factor 8/myostatin, fibroblast growth factor 6 and leukemia inhibitory factor in overloaded, regenerating and denervated rat muscles. Biochim Biophys Acta 2000; 1497: 77-88.
[40] McFarlane C, Plummer E, Thomas M, Hennebry A, Ashby M, Ling N, Smith H, Sharma M and Kambadur R. Myostatin induces cachexia by activating the ubiquitin proteolytic system through an NF-kappaB-independent, FoxO1-dependent mechanism. J Cell Physiol 2006; 209: 501-514.
[41] Tajbakhsh S, Rocancourt D, Cossu G and Buckingham M. Redefining the genetic hierarchies controlling skeletal myogenesis: Pax-3 and Myf-5 act upstream of MyoD. Cell 1997; 89: 127-138.
[42] Hamrick MW. Increased bone mineral density in the femora of GDF8 knockout mice. Anat Rec A Discov Mol Cell Evol Biol 2003; 272: 388-391.
[43] Kellum E, Starr H, Arounleut P, Immel D, Fulzele S, Wenger K and Hamrick MW. Myostatin (GDF-8) deficiency increases fracture callus size, Sox-5 expression, and callus bone volume. Bone 2009; 44: 17-23.
[44] Fiore F, Planche J, Gibier P, Sebille A, deLapeyrière O, Birnbaum D. Apparent normal phenotype of Fgf6-/- mice. Int J Dev Biol 1997; 41: 639-642.
[45] Sakuma K, Watanabe K, Sano M, Uramoto I, Sakamoto K and Totsuka T. The adaptive response of MyoD family proteins in overloaded, regenerating and denervated rat muscles. Biochim Biophys Acta 1999; 1428: 284-292.
[46] Elkasrawy MN and Hamrick MW. Myostatin (GDF-8) as a key factor linking muscle mass and bone structure. J Musculoskelet Neuronal Interact 2010; 10: 56-63.
[47] Jiang WJ, Zhang JA. Calcitriol reduces proteinuria and improves bone mineral density in patients with diabetic nephropathy: a prospective randomized controlled study. Int J Clin Exp Med 2017; 10: 13194-13200.